Obesity and brain topological organization differences throughout the lifespan.

Ottino-González, J.[1,2,3,*], Baggio, H.C.[2,4,*], Jurado, M.A.[1,2,3,✉], Segura, B.[2,4], Caldú, X.[1,2,3], Prats-Soteras, X.[1,2,3], Tor, C.[7], Sender-Palacios, M.J.[7], Miró, N.[6], Sánchez-Garre, C.[6], Dadar, M.[5], Dagher, A.[5], García-García, I.[5], and Garolera, M.[8,9]

[1]Departament de Psicologia Clínica i Psicobiologia. Universitat de Barcelona, Spain.
[2]Institut de Neurociències. Universitat de Barcelona, Spain.
[3]Institut de Recerca Sant Joan de Dèu. Hospital Sant Joan de Dèu, Spain.
[4]Departament de Medicina. Universitat de Barcelona, Spain.
[5]Montreal Neurological Institute. McGill University, Canada.
[6]Unitat de Endocrinologia, Hospital de Terrassa. Consorci Sanitari de Terrassa, Spain.
[7]CAP Terrassa Nord. Consorci Sanitari de Terrassa, Spain.
[8]Unitat de Neuropsicologia, Hospital de Terrassa. Consorci Sanitari de Terrassa, Spain.
[9]Brain, Cognition and Behaviour Research Group. Consorci Sanitari de Terrassa, Spain.
[*]These authors contributed equally to this work.

Abstract – Life expectancy and obesity rates have drastically increased in recent years. An unhealthy weight is related to long-lasting biological deregulations that might jeopardize the so-called "successful aging". Therefore, the principal aim of the current study was to test whether an obesity status could mimic the topological organization of an aged brain. Moreover, we sought to extend literature findings by comparing adults and adolescents with obesity and with normal weight, as well as to explore potential differences in brain maturation in presence of an obesity status. Thus, the current study included adults with (N = 32, mean age 34.5 ± 6.49) and without obesity (N = 34, mean age 32.7 ± 6.79) as well as adolescents with obesity (N = 30, mean age 15.3 ± 2.64) and normal-weight (N = 31, mean age 15.6 ± 2.60). Moreover, a sample of stroke-free non-obese and non-demented seniors was also entered (N = 32, mean age 66.1 ± 7.43). Participants underwent resting-state MRI acquisition and graph-based measurements of segregation, integration and efficiency were calculated. Our results showed that adults with obesity displayed decreases in whole-brain integrity/efficiency (i.e., mean degree and strength) when compared to healthy-weight adults and seniors, as well as increases in network segregation relative to elders. Altogether, this pattern might negatively affect network-resilience and pave the way to an unsuccessful aging of the brain.

Obesity | Aging | Maturation | Resting-state | Graph-theory
Correspondence: ***majurado@ub.edu***

Introduction

Our life expectancy is longer than it has ever been before. Above 30% of the population from Western developed countries will be older than 60 years by 2050 (World Health Organization, 2015). For this reason, research on the psychobiological factors that have an impact on the so-called "successful aging" is rapidly gaining popularity. One of such factors is obesity. The World Health Organization (WHO) estimates that the prevalence of obesity has tripled in the last decades (World Health Organization, 2017). The consequences of obesity involve several chronic conditions, such as type II diabetes, cardiovascular diseases and cancer (Wade, Carslake, Sattar, Davey Smith, & Timpson, 2018). On a similar note, obesity could accelerate brain aging, increasing the risks of suffering late-onset dementia, such as Alzheimer's disease and vascular dementia (Bischof & Park, 2015). The neurobiological mechanisms behind this, however, remain largely elusive. Neuroanatomical studies suggest that obesity is associated with reductions in gray matter volume (García-García et al., 2018) and alterations in white matter microstructure (Repple et al., 2018; Zhang et al., 2018); therefore, an obesity status could be considered as an escalator of brain age (Ronan et al., 2016; Tzanetakou, Katsilambros, Benetos, Mikhailidis, & Perrea, 2012).

The functional organization of the brain is intricate. Distinct and anatomically distant regions interact with each other contributing to cognitive function. Graph-based indexes could serve as proxies of the complex rendering of large-scale networks. Measures of segregation, such as modularity, represent how topologically neighboring brain nodes tend to aggregate as independent clusters (Rubinov & Sporns, 2010). This community-based organization underpins the principle of brain economics where modules specialize onto processing certain sources of information, principally those of sensory nature (Wig, 2017). Integration indexes reflect instead to which extent a priori unrelated modules interchange information. A typical surrogate of integration is the characteristic path length. This parameter reflects the shortest path between modules (Rubinov & Sporns, 2010). Hence, the fewer the jumps, the greater the integration between communities. Well-balanced short and long-range connections allow the rapid combination of resources necessary for higher cognitive activity. Finally, nodal degree and strength mirror the network integrity and efficiency by averaging the amount and the weight of connections a given node has with the rest of the brain (Rubinov & Sporns, 2010). Densely interconnected nodes are metabolically costly and commonly referred to as "hubs" as they exert as bridges coupling remote networks (van den Heuvel & Sporns, 2013).

Aging is associated with losses in the differentiation between well-defined circuits. In other words, nodes that belong to independent communities in younger adults tend to enhance their communications in older adults. These losses in network discreteness could expose either the recruitment

DRAFT

of age-related compensatory mechanisms (Geerligs, Renken, Saliasi, Maurits, & Lorist, 2015), the decreases in the number of nodes and short-range connections (Sala-Llonch et al., 2014), or both. Studies in obesity, however, are not so clear as to whether this condition is related to changes that resemble those observed in aging individuals (Beyer et al., 2017; Doucet, Rasgon, McEwen, Micali, & Frangou, 2017).

To date, and to the best of our knowledge, only three studies have explored the brain functional organization in obese individuals with graph-theoretical parameters. Two works reported lower modularity in individuals with obesity when compared to healthy-weight subjects (Baek, Morris, Kundu, & Voon, 2017; Chao et al., 2018). A third study described global brain connectivity decreases mainly within prefrontal circuits (Geha, Cecchi, Todd Constable, Abdallah, & Small, 2017). The current study had two aims. The first and main objective was to explore whether an obesity status is linked to brain connectivity patterns similar to those present in elders. To achieve this, we matched adults with and without obesity and non-obese healthy seniors. The second aim was to examine if an obesity condition could differently shape the brain functional topological organization during development. To answer this, we tested for interactions between body-weight status in adults and adolescents.

Methods

Participants. Two independently collected samples were included in this work. One sample comprised 32 non-obese healthy seniors (51-85 years old). The recruitment procedure of this group is fully described in Abós et al. (2017). Briefly, exclusion criteria consisted on presence of psychiatric or neurological comorbidity, low global intelligence quotient estimated by the WAIS-III Vocabulary subtest score (> 7 scalar score) (Wechsler, 1999), and a Mini-Mental state examination score below 25 (Folstein, Folstein, & McHugh, 1975). For the current work, senior participants with obesity were excluded (N = 4) as well as those presenting MRI pathological findings such as white matter hyperintensities unrelated to the course of normal aging (N = 2).

The other sample included 61 adolescents (12-21 years old) and 66 adults (22-48 years old) from public health care centers belonging to the *Consorci Sanitari de Terrassa*. This sample was recruited in the context of a broader line of research revolving around obesity and brain function. Part of this sample was used in previous works (Ariza et al., 2012; Caldú et al., 2019; García-García et al., 2013a, 2013b, 2013c, 2015; Marqués-Iturria et al., 2013, 2014, 2015; Ottino-González et al., 2017, 2018, 2019). Following the cut-offs established by the WHO (2012), 32 adults with a body mass index (BMI) equal to or higher than 30 kg/m^2 and 30 adolescents above the gender-based 95th BMI percentile were categorized as obese (Cole, Flegal, Nicholls, & Jackson, 2007). Similarly, 34 adults with a BMI ranging from 18.5 to 24.9 kg/m^2, and 31 teens oscillating between the 5th and the 84th percentile, were categorized as healthy-weight. Thirty-four individuals with overweight (i.e., BMI 25 to 29.9 kg/m^2 or between the 85th and 94th percentiles) were not included in this study since we were only interested in addressing the two extremes of the BMI continuum.

As in previous work, we excluded participants with cardiometabolic comorbidities (i.e., type II diabetes, hypercholesterolemia, hypertension), as well as those with past or present neurological or psychiatric disorders. Individuals underwent three visits. The first consisted of a fasting blood sample extraction and a medical exploration. The second visit included an extensive neuropsychological evaluation in which subjects with a Vocabulary subtest scalar score below 7 were discarded (WAIS-III or WISC-IV) (Wechsler, 1999, 2007). The third and last visit comprised a magnetic resonance imaging (MRI) acquisition at the *Hospital Clínic de Barcelona*.

Additionally, participants from all five groups exhibiting excessive head motion were discarded (N = 16). Excessive movement was defined as (1) mean interframe head motion greater than 0.3 mm translation or 0.3° rotation, and (2) maximum interframe head motion greater than 1 mm translation or 1° rotation.

MRI acquisition. Images were acquired with a 3T Siemens scanner (MAGNETOM Trio, Siemens, Germany). Each participant underwent a T1-weighted structural image for co-registration and parcellation purposes with the MPRAGE-3D protocol [echo time (TE) = 2.98 ms; repetition time (TR) = 2300 ms; inversion time = 900 ms; 256 mm field of view [FOV]; matrix size = 256 x 256; voxel size = 1.0 x 1.0 x 1.0 mm^3). Resting-state volumes in adolescents and adults were collected using a multi-slice gradient-echo EPI sequence covering the whole brain (TE = 19 ms; TR = 2000 ms; 3 mm slice thickness; 90° flip angle; 220 mm FOV; voxel size = 1.7 x 1.7 x 3.0 mm^3). Resting-state images in the elders were obtained with the following parameters: TE = 28 ms, TR = 2500 ms, 80° flip angle, 3 mm slice thickness, 240 mm FOV, voxel size = 1.7 x 1.7 x 3.0 mm^3.

Image pre-processing. Basic functional image preprocessing, using AFNI (http://afni.nimh.nih.gov/afni) and FSL (https://www.fmrib.ox.ac.uk/fsl) tools, included: discarding the first five volumes to allow magnetization stabilization, despiking, motion correction, brain extraction, grand-mean scaling, linear detrending, and high-pass filtering (maintaining frequencies above 0.01 Hz). Functional images and T1-weighted volumes were co-registered and then non-linearly normalized to the MNI ICBM152 template. The resulting preprocessed images were therefore non-linearly transformed to MNI space at 3 x 3 x 3 mm^3 voxel size using SPM (http://www.fil.ion.ucl.ac.uk/spm/).

To remove the effects of head motion and other non-neural sources of signal variation from the functional data sets, we used an independent component analysis (ICA)-based strategy for Automatic Removal of Motion Artifacts (ICA-AROMA) (Pruim et al., 2015). This method uses individual resting-state data to perform ICAs and automatically identify artifact-related independent components. The time courses of components considered as artifactual were stored to be used as regressors during network computation.

DRAFT

The six motion parameters obtained from the realignment procedure, as well as the average white matter and cerebrospinal fluid signals were stored to serve as regressors in network reconstruction. To generate the corresponding white matter and cerebrospinal fluid (lateral ventricle) masks, T1-weighted structural images were segmented using FreeSurfer (https://surfer.nmr.mgh.harvard.edu/). The resulting binary masks were linearly transformed from structural to native functional space using FSL-FLIRT (https://fsl.fmrib.ox.ac.uk/fsl/fslwiki/FLIRT). To prevent these masks from extending to the adjacent gray matter due to resampling blur in linear transformation, white matter masks were then "eroded" by applying a threshold of 0.9, while ventricular masks were thresholded at 0.3.

Connectivity matrix computation. To reconstruct the functional connectome, the brain needs to be divided into a set of nodes; network edges connecting pairs of nodes are then defined as a measure of relationship between their respective time courses. In this work, we used the Brainnetome atlas (Fan et al., 2016), a cross-validated connectivity-based parcellation scheme that divides the cerebrum into 210 cortical and 36 subcortical gray matter regions, taken as network nodes. The first eigenvariates of the time series of all voxels included in each region mask were extracted using *fslmeants* and taken as the time course of the corresponding nodes.
Individual 246 x 246 connectivity matrices were then reconstructed by calculating the standardized regression coefficient between the time courses of nodes *i* and *j*, while also entering the ICA-AROMA artifact time courses, six motion parameters, and white matter and cerebrospinal fluid mean time courses as regressors. This produces fully connected and undirected brain networks with 30,135 unique edges with values ranging between -1 and 1.
Moreover, a group temporal-concatenation spatial ICA was performed using FSL's MELODIC (https://fsl.fmrib.ox.ac.uk/fsl/fslwiki/MELODIC) with a pre-determined dimensionality of 15 independent components. The spatial and power spectral characteristics of the resulting components were inspected to identify 10 well-established networks (Griffanti et al., 2017): two primary visual networks (PVN and PVN2), secondary visual network (SVN), default mode network (DMN), dorsal attentional network (DAN), anterior default mode network (aDMN), right and left frontoparietal networks (FPN), sensory-motor network (SMN) and the salience network (SN) (see Supplementary Figure 1). Two additional networks were identified as the medial temporal network (MTN) (including the hippocampus and the amygdala) and the striatal-thalamic network (STN).
These data-driven spatial maps were used to assign the Brainnetome's nodes to specific brain networks for further regional graph-based measurements calculation, using in-house MATLAB scripts. Specifically, the Z-maps generated by MELODIC corresponding to the 12 networks of interest were thresholded at $Z \geq 2$. Subsequently, each Brainnetome node was considered to belong to a network if over 60% of its voxels overlapped with this network's thresholded map. When this overlap occurred for more than one network, the sum of the Z-values across all overlapping voxels was considered, and the node was assigned to the network with the highest Z-value sum. In total, 153 of the 246 Brainnetome nodes were ascribed to one of the 12 networks of interest, as shown in Supplementary Table 1.

Global and regional graph-theory parameters estimation. Global network parameters were computed using the Brain Connectivity Toolbox (Rubinov & Sporns, 2010) and in-house MATLAB scripts. As non-normalized global parameters, we assessed two complementary metrics: the mean network degree (average number of positive connections linked to a node, across all brain nodes) and the mean network strength (average of unthresholded connection strength across all edges, positive and negative), both of which can be understood as measures of network efficiency and integrity. We also computed the modularity coefficient, calculated using the Louvain algorithm and indicating the degree to which a network can be subdivided into well-defined modules with few intermodular connections. We also calculated normalized weighted global measures by averaging the ratio between the actual measures and those obtained through randomly rewiring the connectivity matrix 500 times using a degree-preserving algorithm. Thus, after setting negative edge weights to zero, we computed the characteristic path length, defined as the average minimum number of edges that need to be traversed between each pair of network nodes (Rubinov & Sporns, 2010). Regional network parameters such as degree and strength were calculated by averaging the total number of connections and weights between nodes ascribed to each ICA-based network and the rest of the brain.

Statistical analysis

Sociodemographic variables as well as the mean interframe translational and rotational movements of the head were examined across groups. Non-parametrical tests were applied when data assumptions were violated. All comparisons of global and regional graph-based measures were conducted with permutation-based tests (10,000 permutations). One-factor univariate general linear models (GLMs) were conducted in adults and seniors. To avoid comparisons of non-interest, differences in adolescents were tested in independent models. Post-hoc pairwise permutation t-tests were performed for contrasts that emerged as statistically significant. Cumulative odds for false-positive results were prevented with Bonferroni-adjustments. Here, the raw p-values were multiplied by *k* variables for omnibus tests (i.e., by 4 for global graph-based measures, and by 12 for regional degree and strength parameters), and by *n* contrast of interest (3) in post-hoc comparisons. Statistical significance was set at adjusted p-value < 0.05. Likewise, effect sizes (i.e., Cohen's d or eta-partial square [ηp^2]) and bias-corrected and accelerated bootstrap (10,000 simulations) confidence intervals (CI 95%, or 90% for ηp^2) were calculated for each significant pairwise contrast. Moreover, to explore for differences in the transition from young to adulthood in both global and

DRAFT

Table 1. Sociodemographics across groups (mean and standard deviation)

Groups	Age	Education	Females
OB adult	34.53 (6.49)	13.88 (2.92)	20 (62.5%)
HW adult	32.68 (6.79)	14.62 (2.75)	18 (52.9%)
Senior	66.13 (7.43)	11.22 (4.26)	17 (53.13%)
OB young	15.27 (2.64)	8.57 (2.45)	15 (50%)
HW young	15.64 (2.60)	9.52 (2.19)	16 (51.6%)

OB = participant with obesity, HW = healthy-weight individual.

regional graph-related indexes, we sought for interactions between body-weight status (i.e., healthy-weight vs. obesity) and age (i.e., adolescent vs. adult) with permutation-based two-factor univariate GLMs. All statistical analyses were performed with *R* version 3.5.0 (R Core Team, 2018).

Results

Sociodemographics. As expected, groups differed in age ($F_{(4,153)} = 420$, $p < 0.001$) and years of education ($F_{(4,153)} = 24.62$ $p < 0.001$). Post-hoc analyses revealed no significant differences between adults with and without obesity in age (p-adjusted = 0.674) or education (p-adjusted = 0.854). Similarly, healthy-weight and obese adolescents were comparable in terms of age (p-adjusted = 0.999) and years of education (p-adjusted = 0.732). All five groups were equally distributed for sex ($x^2 = 1.22$, $p = 0.875$) (Table 1).

MRI quality check. Rotational movements of the head did not diverge between groups ($H_{(4)} = 4.32$, $p = 0.364$). By contrast, head translational movements proved different among groups ($H_{(4)} = 38.90$, $p < 0.001$), with post-hoc analyses revealing that such displacements were more marked for elders and adults with obesity, as both of them differed from the other groups yet not from each other. Consequently, head translational movements were controlled for all further graph-theoretical analyses, either by introducing it as a covariate or adjusting each variable of interest by the standardized residual method.

Global graph-based results. Adults and seniors exhibited differences in modularity ($F_{(3,94)} = 5.71$, p-adjusted = 0.016), mean degree ($F_{(3,94)} = 5.56$, p-adjusted = 0.024), and mean strength ($F_{(3,94)} = 4.81$, p-adjusted = 0.040).
Post-hoc analyses exposed that adults with obesity showed lower mean degree ($t = 2.69$, p-adjusted = 0.016, $d = -0.66$; CI_{bca}95% [-1.11, -0.12]) and mean strength ($t = 2.74$, p-adjusted = 0.014, $d = -0.68$; CI_{bca}95% [-1.11, -0.20]) when compared to their normal-weight counterparts. Modularity results did not pass the Bonferroni adjustment (raw p-value = 0.021) in this comparison. Relative to seniors, adults with obesity presented greater modularity ($t = -3.94$, p-adjusted = 0.003, $d = 0.99$; CI_{bca}95% [0.42, 1.55]), as well as lower mean degree ($t = 3.38$, p-adjusted = 0.003, $d = -0.85$; CI_{bca}95% [-1.33, -0.36]) and strength ($t = 2.81$, p-adjusted = 0.025, $d = -0.70$; CI_{bca}95% [-1.15, -0.21]). Normal-weight adults did not differ from non-obese elders for any of the abovementioned indexes. Results are depicted below in Figure 1.

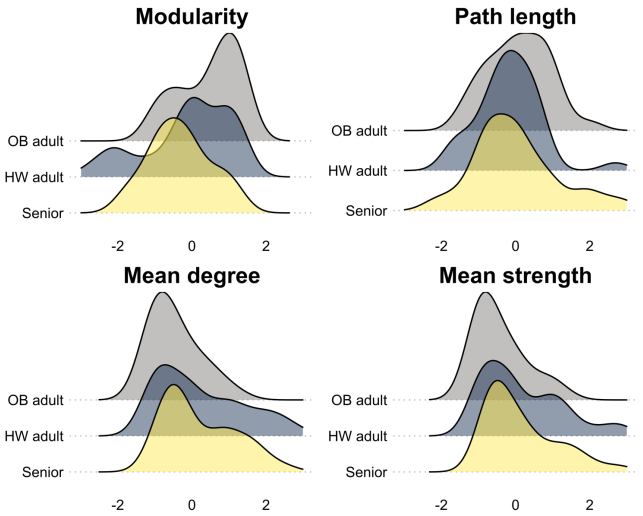

Figure 1. Probability density function of global graph-theoretical parameters in adults. OB = participants with obesity, HW = healthy-weight individuals.

Furthermore, adolescents with and without obesity did not diverge from each other for any graph-related indexes as portrayed in Figure 2. Additionally, mean and standard deviation across groups for graph-based parameters are included in the Supplementary Table 2.

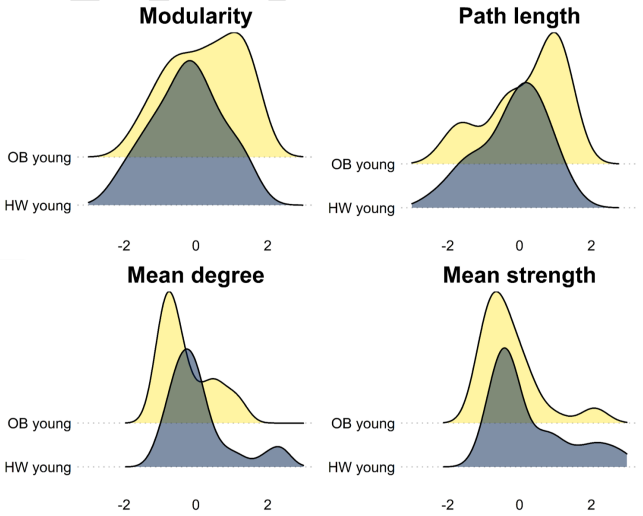

Figure 2. Probability density function of global graph-theoretical parameters in adolescents. OB = participants with obesity, HW = healthy-weight individuals.

Regional nodal degree and strength results. Groups diverged in the average number of inward and outward connections in the DMN ($F_{(3,94)} = 5.97$, p-adjusted = 0.035) and the SMN ($F_{(3,94)} = 6.61$, p-adjusted = 0.007).
Post-hoc tests showed that adults with obesity displayed lesser regional degree than healthy-weight adults in the DMN ($t = 3.21$, p-adjusted = 0.011, $d = -0.79$; CI_{bca}95% [-1.26, -0.33]) and in the SMN ($t = 3.45$, p-adjusted = 0.002, $d = -0.85$; CI_{bca}95% [-1.34, -0.34]). When compared to non-obese elders, adults with obesity only demonstrated lower degree in the DMN ($t = 3.15$, p-adjusted = 0.007, $d = -0.79$; CI_{bca}95% [-1.26, -0.28]). SMN results did not survive the Bonferroni adjustment (raw p-value = 0.041).

DRAFT

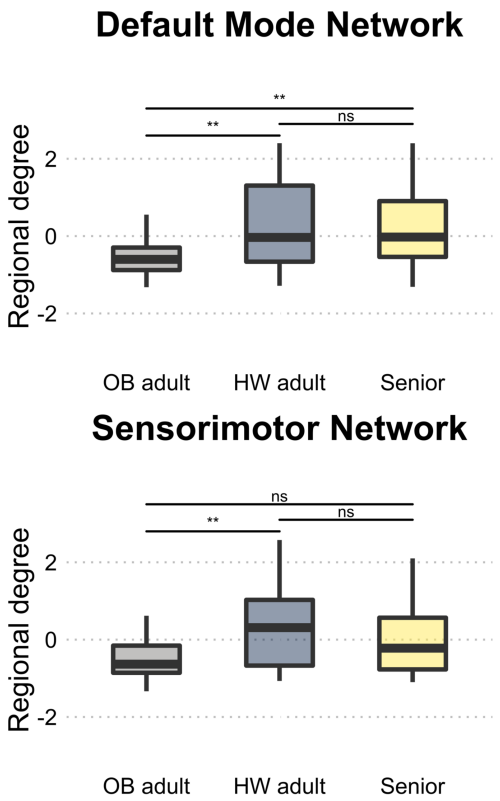

Figure 3. Group comparison for regional nodal degree in specific large-scale networks. OB = participants with obesity, HW = healthy-weight individuals, *<0.05, **<0.01, ns = non-significant.

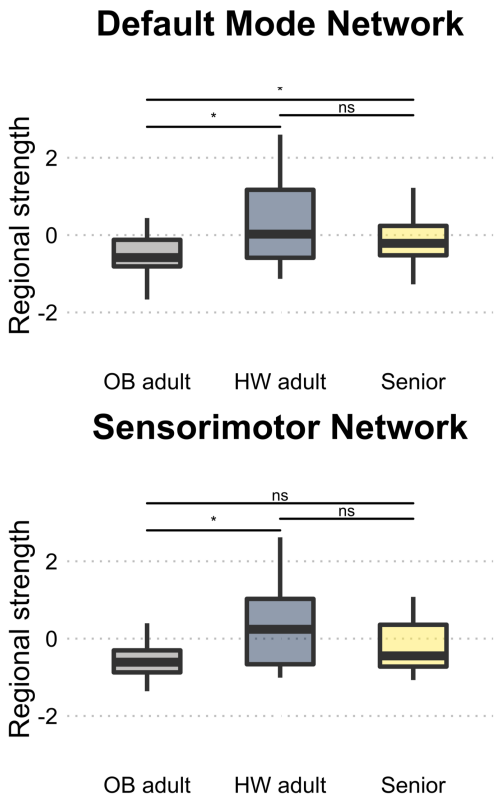

Figure 4. Group comparison for regional nodal strength in specific large-scale networks. OB = participants with obesity, HW = healthy-weight individuals, *<0.05, **<0.01, ns = non-significant.

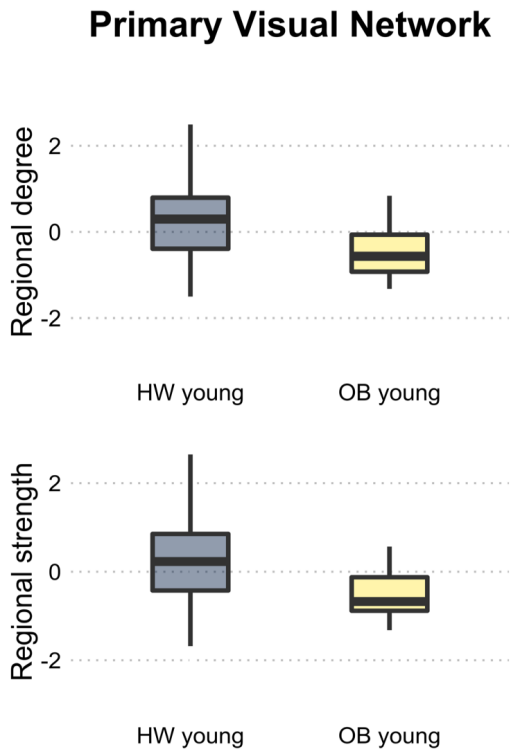

Figure 5. Group comparison for regional nodal degree and strength in the Primary Visual Network. OB = participants with obesity, HW = healthy-weight individuals, *<0.05, **<0.01, ns = non-significant.

As for the regional strength of large-scale networks, the three groups revealed differences, again, among the DMN ($F_{(3,94)}$ = 7.02, p-adjusted = 0.022) and the SMN ($F_{(3,94)}$ = 6.23, p-adjusted = 0.032).

Post-hoc contrasts elicited that adults with obesity demonstrated lesser strength in the DMN (t = 3.67, p-adjusted = 0.001, d = -0.90; CI_{bca}95% [-1.33, -0.44] and the SMN (t = 3.54, p-adjusted = 0.002, d = -0.87; CI_{bca}95% [-1.37, -0.39]) when rivalled to healthy-weight adults. In comparison to elders, adults with obesity also proved a weakening in the weight of connections within the DMN and the rest of the brain (t = 2.57, p-adjusted = 0.031, d = -0.64; CI_{bca}95% [-1.03, -0.17]). Normal-weight adults did not diverge from elders. Regional degree and strength results are available in Figure 3 and Figure 4, respectively.

Adolescents with and without obesity only proved different in the regional degree ($F_{(2,58)}$ = 8.99, p-adjusted = 0.048, ηp^2 = 0.13; [0.02, 0.27]) and strength ($F_{(2,58)}$ = 9.92, p-adjusted = 0.024, ηp^2 = 0.15; [0.019, 0.29]) of the PVN, as illustrated in Figure 5.

Body-weight status and age interaction. There were no significant interactions between body-weight status and age for any graph-theoretical measurement as presented in Figure 6. No interaction for regional degree nor strength emerged as significant either.

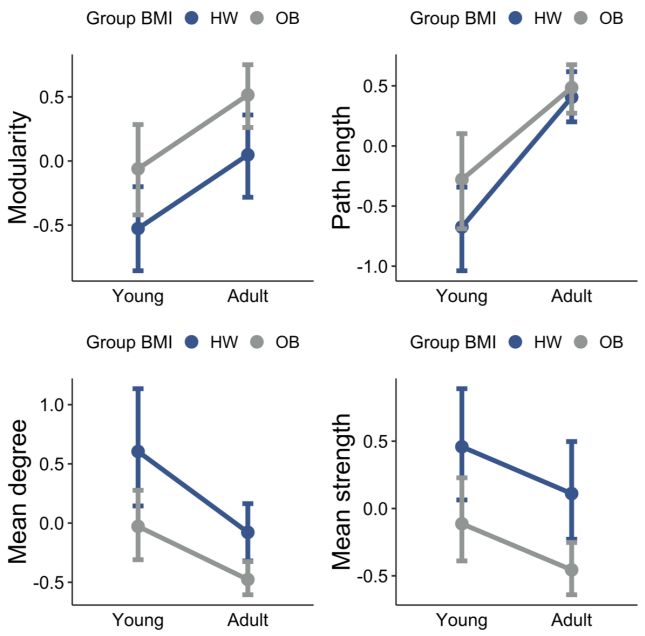

Figure 6. Age and body-weight status interactions for global graph-related indexes. OB = participants with obesity, HW = healthy-weight individuals.

Discussion

The current work aimed to shed a broader light on whether an obesity status could be related to changes on how the brain is functionally organized. We found that groups differed in global graph-based parameters. Adults with obesity exhibited increased lower mean degree and mean strength when compared to healthy-weight adults and non-obese elders. Moreover, this group also demonstrated greater modularity in comparison to non-obese elders. Normal-weight adults did not diverge from seniors for any graph-theoretical parameter. Although adolescents with and without obesity did not differ for global graph-based indexes, they showed differences in the regional degree and strength of visual networks. In addition, no interaction emerged between body-weight status and age for any of these variables.

Modularity. This index can be generally regarded as a proxy of network segregation, which stands for how clustered the brain is in terms of sharing and processing information (Sporns, 2013). As the brain ages, modularity tends to decrease as a result of the progressive scattering of intra-network pairwise connections (Geerligs et al., 2015; Sala-Llonch, Bartrés-Faz, & Junqué, 2015; Sala-Llonch et al., 2014). Our finding of higher modularity in obesity relative to seniors (and healthy-weight adults to some extent) might reflect that the information is densely handled within clusters rather than be generally distributed. Although this could benefit the processing of sensory-specific information, higher-level cognitive activity may deteriorate from an overly modular brain organization (Sporns, 2013). In addition, an increase in segregation could entail a risk factor for the development of disconnection syndromes in the face of cardiovascular insults as with stroke and aphasia (Siegel et al., 2018).

Global and regional mean degree and strength. These parameters respectively echo the number of edges connected to a given node and the average weight of such links. Therefore, both return a global reading of the network efficiency and integrity. One of the consequences of aging on the brain is the trimming of short-range edges and the scattering of nodes (Sala-Llonch et al., 2014). Our results showed that adults with obesity presented a lower mean degree and mean network strength when compared to healthy-weight adults and seniors. These results are partially in line with the study conducted by Geha et al. (2017). In this work, the authors served a measure of global brain connectivity, defined as the number of connections each node has with others. Altogether, global decreases in mean degree and strength in obesity could mirror the loses in network robustness already described occurring in aging.

What is more, when examined regionally, we found group differences in sensory-driven circuits (i.e., SMN), as well as in task-negative networks (i.e., DMN). Overall, these findings support the idea of network-resilience weakening. Also, adolescents with obesity presented lower degree and strength in visual networks. Sensory-processing circuits are naturally engaged during the handling of domain-specific information. It is described that subjects with obesity feature alterations within tactile and visual-processing networks (Doucet et al., 2017; García-García et al., 2013; Geha et al., 2017). The DMN, the most typical task-negative network, is considered to be a biomarker for pathological aging and dementia (Buckner, Andrews-Hanna, & Schacter, 2008; Palmqvist et al., 2017). This network is also extremely vulnerable to the negative effects of obesity-related disorders such as type II diabetes (Wang, Ji, Lu, & Zhang, 2016), hypertension (Haight et al., 2015), and dyslipidemia (Spielberg et al., 2017). To date, very few studies have described alterations in the DMN relative to an obesity status (Beyer et al., 2017; Doucet et al., 2017; Figley, Asem, Levenbaum, & Courtney, 2016; Tregellas et al., 2011).

Obesity is a preventable health problem associated with the development of long-lasting cardiometabolic disorders (Wade et al., 2018). This condition is related to a status of low-grade chronic inflammation presumably responsible for such medical complications (Ellulu, Patimah, Khaza'ai, Rahmat, & Abed, 2017). Likewise, aging is also linked to sustained, yet sterile, inflammation potentially contributing to insulin resistance development and weight-gain (Frasca, Blomberg, & Paganelli, 2017). To date, the pathological source underlying the brain changes described in subjects with obesity is unknown. It is nevertheless remarkable that both conditions are linked to a pro-inflammatory milieu, and that by the same token, the two can influence each other (Spencer et al., 2017; Valcarcel-Ares et al., 2019). Relative to non-obese elders, adults with obesity exhibited an increase in the network segregation that was also associated with a reduction in the number and weight of connections. Altogether, this pattern of brain organization could entail an increased vulnerability to cardiovascular deregulations that might start to aggregate over the years as long as this condition remains

DRAFT

unsolved.

The current work has limitations that should be accounted for in future studies. First, its cross-sectional nature prevents to draw any conclusion upon causality. Longitudinal approaches would help disentangle whether the transition from adulthood to elderhood in the same group of individuals is different in the presence of an unhealthy weight. This limitation also applies to the brain maturation issue. Second, our modest sample size (N = 159) might have limited our statistical power to catch any subtle difference. Third, to have had a group of elders with obesity would have allowed exploring the impact of such condition across all possible age ranges. Fourth, the resting-state acquisition in the senior cohort were slightly different from the rest of the groups, which is something that should be taken into account. By contrast, a strong point of this work was the strict criteria that ruled out participants with neurological or psychiatric comorbidities likely prompting network-related differences.

In sum, adults with obesity have showed differences in graph-based measures of network organization. Concretely, and compared to healthy-weight adults and non-obese seniors, volunteers with obesity demonstrated a pattern of losses in network integrity and efficiency. What is more, adults with obesity exhibited increases in brain segregation relative to seniors. Overall, these findings could point towards a weakening in network resilience that might jeopardize the so-called "successful aging".

Bibliography

1. A. Abós, H Baggio, B. Segura, A.I. García-Díaz, Y. Compta, M.J. Martí, F. Valldeoriola, and C. Junqué. Discriminating cognitive status in Parkinson's disease through functional connectomics and machine learning. *Scientific Reports*, 7(1):45347, 12 2017. ISSN 2045-2322. doi: 10.1038/srep45347.
2. M. Ariza, M. Garolera, M.A. Jurado, I. Garcia-Garcia, I. Hernan, C. Sánchez-Garre, M. Vernet-Vernet, M.J. Sender-Palacios, I. Marques-Iturria, R. Pueyo, B. Segura, and A. Narberhaus. Dopamine Genes (DRD2/ANKK1-TaqA1 and DRD4-7R) and Executive Function: Their Interaction with Obesity. *PLoS ONE*, 7(7):e41482, 1 2012. ISSN 1932-6203; 1932-6203. doi: 10.1371/journal.pone.0041482.
3. K. Baek, L. S. Morris, P. Kundu, and V. Voon. Disrupted resting-state brain network properties in obesity: Decreased global and putaminal cortico-striatal network efficiency. *Psychological Medicine*, 47(4):585–596, 2017. ISSN 14698978. doi: 10.1017/S0033291716002646.
4. F. Beyer, S. Kharabian Masouleh, J.M. Huntenburg, L. Lampe, T. Luck, S.G. Riedel-Heller, M. Loeffler, M.L. Schroeter, M. Stumvoll, A. Villringer, and A.V. Witte. Higher body mass index is associated with reduced posterior default mode connectivity in older adults. *Human Brain Mapping*, 3515(April):3502–3515, 2017. ISSN 10970193. doi: 10.1002/hbm.23605.
5. G.N. Bischof and D.C. Park. Obesity and Aging. *Psychosomatic Medicine*, 77(6):697–709, 1 2015. ISSN 0033-3174. doi: 10.1097/PSY.0000000000000212.
6. R.L. Buckner, J.R. Andrews-Hanna, and D.L. Schacter. The brain's default network: Anatomy, function, and relevance to disease. *Annals of the New York Academy of Sciences*, 1124:1–38, 2008. ISSN 00778923. doi: 10.1196/annals.1440.011.
7. X. Caldú, J. Ottino-González, C. Sánchez-Garre, I. Hernan, E. Tor, M.J. Sender-Palacios, J.C. Dreher, M. Garolera, and M.A. Jurado. Effect of the catechol- O -methyltransferase Val 158 Met polymorphism on theory of mind in obesity. *European Eating Disorders Review*, (August 2018):1–9, 2 2019. ISSN 10724133. doi: 10.1002/erv.2665.
8. S.H. Chao, Y.T. Liao, V.C.H. Chen, C.J. Li, R.S. McIntyre, Y. Lee, and J.C. Weng. Correlation between brain circuit segregation and obesity. *Behavioural Brain Research*, 337(259):218–227, 2018. ISSN 18727549. doi: 10.1016/j.bbr.2017.09.017.
9. T.J Cole, K.M Flegal, S. Nicholls, and A.A Jackson. Body mass index cut offs to define thinness in children and adolescents: international survey. *BMJ (Clinical research ed.)*, 335 (7612):194, 7 2007. ISSN 1468-5833. doi: 10.1136/bmj.39238.399444.55.
10. G.E. Doucet, N. Rasgon, B.S. McEwen, N. Micali, and S. Frangou. Elevated Body Mass Index is Associated with Increased Integration and Reduced Cohesion of Sensory-Driven and Internally Guided Resting-State Functional Brain Networks. *Cerebral Cortex*, (April): 988–997, 2017. ISSN 1047-3211. doi: 10.1093/cercor/bhx008.
11. M.S. Ellulu, I. Patimah, H. Khaza'ai, A. Rahmat, and Y. Abed. Obesity and inflammation: the linking mechanism and the complications. *Archives of Medical Science*, 4:851–863, 2017. ISSN 1734-1922. doi: 10.5114/aoms.2016.58928.
12. L. Fan, H. Li, J. Zhuo, Y. Zhang, J. Wang, L. Chen, Z. Yang, C. Chu, S. Xie, A.R. Laird, P.T. Fox, S.B. Eickhoff, C. Yu, and T. Jiang. The Human Brainnetome Atlas: A New Brain Atlas Based on Connectional Architecture. *Cerebral Cortex*, 26(8):3508–3526, 8 2016. ISSN 1047-3211. doi: 10.1093/cercor/bhw157.
13. C.R. Figley, J.S.A. Asem, E.L. Levenbaum, and S.M. Courtney. Effects of body mass index and body fat percent on default mode, executive control, and salience network structure and function. *Frontiers in Neuroscience*, 10(June):1–23, 2016. ISSN 1662-453X. doi: 10.3389/fnins.2016.00234.
14. M.F. Folstein, S.E. Folstein, and P.R. McHugh. "Mini-mental state": A practical method for grading the cognitive state of patients for the clinician. *Journal of Psychiatric Research*, 12 (3):189–198, 11 1975. ISSN 00223956. doi: 10.1016/0022-3956(75)90026-6.
15. D. Frasca, B.B. Blomberg, and R. Paganelli. Aging, obesity, and inflammatory age-related diseases. *Frontiers in Immunology*, 8(DEC):1–10, 2017. ISSN 16643224. doi: 10.3389/fimmu.2017.01745.
16. I. García-García, A. Narberhaus, I. Marqués-Iturria, M. Garolera, A. Rădoi, B. Segura, R. Pueyo, M. Ariza, and M. A. Jurado. Neural Responses to Visual Food Cues: Insights from Functional Magnetic Resonance Imaging. *European Eating Disorders Review*, 21(2): 89–98, 3 2013. ISSN 10724133. doi: 10.1002/erv.2216.
17. I. García-García, M.A. Jurado, M Garolera, B Segura, I Marqués-Iturria, R Pueyo, M Vernet-Vernet, M.J. Sender-Palacios, R Sala-Llonch, M Ariza, A Narberhaus, and C Junqué. Functional connectivity in obesity during reward processing. *NeuroImage*, 66:232–239, 2 2013. ISSN 10538119. doi: 10.1016/j.neuroimage.2012.10.035.
18. I. García-García, M.A. Jurado, M. Garolera, B. Segura, R. Sala-Llonch, I. Marqués-Iturria, R. Pueyo, M.J. Sender-Palacios, M. Vernet-Vernet, A. Narberhaus, M. Ariza, and C. Junqué. Alterations of the salience network in obesity: A resting-state fMRI study. *Human Brain Mapping*, 34(11):2786–2797, 11 2013. ISSN 10659471. doi: 10.1002/hbm.22104.
19. I. García-García, M.A. Jurado, M. Garolera, I. Marqués-Iturria, A. Horstmann, B. Segura, R. Pueyo, M.J. Sender-Palacios, M. Vernet-Vernet, A. Villringer, C. Junqué, D.S. Margulies, and J. Neumann. Functional network centrality in obesity: A resting-state and task fMRI study. *Psychiatry Research: Neuroimaging*, 233(3):331–338, 9 2015. ISSN 09254927. doi: 10.1016/j.pscychresns.2015.05.017.
20. I. García-García, A. Michaud, M. Dadar, Y. Zeighami, S. Neseliler, D.L Collins, A.C. Evans, and A. Dagher. Neuroanatomical differences in obesity: meta-analytic findings and their validation in an independent dataset. *International Journal of Obesity*, 9, 7 2018. ISSN 0307-0565. doi: 10.1038/s41366-018-0164-4.
21. L. Geerligs, R.J. Renken, E. Saliasi, N.M. Maurits, and M.M. Lorist. A Brain-Wide Study of Age-Related Changes in Functional Connectivity. *Cerebral Cortex*, 25(7):1987–1999, 7 2015. ISSN 1460-2199. doi: 10.1093/cercor/bhu012.
22. P. Geha, G. Cecchi, Todd C.R., C. Abdallah, and D.M. Small. Reorganization of brain connectivity in obesity. *Human Brain Mapping*, 38(3):1403–1420, 3 2017. ISSN 10659471. doi: 10.1002/hbm.23462.
23. L. Griffanti, G. Douaud, J. Bijsterbosch, S. Evangelisti, F. Alfaro-Almagro, M.F. Glasser, E.P. Duff, S. Fitzgibbon, R. Westphal, D. Carone, C.F. Beckmann, and S.M. Smith. Hand classification of fMRI ICA noise components. *NeuroImage*, 154(June 2016):188–205, 2017. ISSN 10959572. doi: 10.1016/j.neuroimage.2016.12.036.
24. T.J. Haight, R.N. Bryan, G. Erus, C. Davatzikos, D.R. Jacobs, M. D'Esposito, C.E. Lewis, and L.J. Launer. Vascular risk factors, cerebrovascular reactivity, and the default-mode brain network. *NeuroImage*, 115:7–16, 2015. ISSN 10959572. doi: 10.1016/j.neuroimage.2015.04.039.
25. I. Marqués-Iturria, R. Pueyo, M. Garolera, B. Segura, C. Junqué, I. García-García, M.J. Sender-Palacios, M. Vernet-Vernet, A. Narberhaus, M. Ariza, and M.A. Jurado. Frontal cortical thinning and subcortical volume reductions in early adulthood obesity. *Psychiatry Research: Neuroimaging*, 214(2):109–115, 11 2013. ISSN 09254927. doi: 10.1016/j.pscychresns.2013.06.004.
26. I. Marqués-Iturria, M. Garolera, R. Pueyo, B. Segura, I. Hernan, I. García-García, C. Sánchez-Garre, M. Vernet-Vernet, M.J. Sender-Palacios, A. Narberhaus, M. Ariza, C. Junqué, and M.A. Jurado. The interaction effect between BDNF val66met polymorphism and obesity on executive functions and frontal structure. *American Journal of Medical Genetics Part B: Neuropsychiatric Genetics*, 165(3):245–253, 4 2014. ISSN 15524841. doi: 10.1002/ajmg.b.32229.
27. I. Marqués-Iturria, L.H. Scholtens, M. Garolera, R. Pueyo, I. García-García, P. González-Tartiere, B. Segura, C. Junqué, M.J. Sender-Palacios, M. Vernet-Vernet, C. Sánchez-Garre, M.A. de Reus, M.A. Jurado, and M.P. van den Heuvel. Affected connectivity organization of the reward system structure in obesity. *NeuroImage*, 111:100–106, 5 2015. ISSN 10538119. doi: 10.1016/j.neuroimage.2015.02.012.
28. J. Ottino-González, M.A. Jurado, I. García-García, X. Caldú, X. Prats-Soteras, E. Tor, M.J. Sender-Palacios, and M. Garolera. Allostatic load and executive functions in overweight adults. *Psychoneuroendocrinology*, 106(April):165–170, 8 2019. ISSN 03064530. doi: 10.1016/j.psyneuen.2019.04.009.
29. J. Ottino-González, M A Jurado, I. García-García, B Segura, I. Marqués-Iturria, M. J. Sender-Palacios, E. Tor, X. Prats-Soteras, X. Caldú, C. Junqué, O. Pasternak, and M. Garolera. Allostatic load and disordered white matter microstructure in overweight adults. *Scientific Reports*, 8(1):15898, 12 2018. ISSN 2045-2322. doi: 10.1038/s41598-018-34219-8.
30. J. Ottino-González, M.A. Jurado, I. García-García, B. Segura, I. Marqués-Iturria, M.J. Sender-Palacios, E. Tor, X. Prats-Soteras, X. Caldú, C. Junqué, and M. Garolera. Allostatic Load Is Linked to Cortical Thickness Changes Depending on Body-Weight Status. *Frontiers in Human Neuroscience*, 11(December):1–11, 12 2017. ISSN 1662-5161. doi: 10.3389/fnhum.2017.00639.
31. S. Palmqvist, M. Schöll, O. Strandberg, N. Mattsson, E. Stomrud, H. Zetterberg, K. Blennow, S. Landau, W. Jagust, and O. Hansson. Earliest accumulation of β-amyloid occurs within the default-mode network and concurrently affects brain connectivity. *Nature Communications*, 8(1):1214, 12 2017. ISSN 2041-1723. doi: 10.1038/s41467-017-01150-x.
32. R.H.R. Pruim, M. Mennes, D. van Rooij, A. Llera, J.K. Buitelaar, and C.F. Beckmann. ICA-AROMA: A robust ICA-based strategy for removing motion artifacts from fMRI data. *NeuroImage*, 112:267–277, 5 2015. ISSN 10538119. doi: 10.1016/j.neuroimage.2015.02.064.
33. R Core Team. R: A Language and Environment for Statistical Computing, 2018.
34. J. Repple, N. Opel, S. Meinert, R. Redlich, T. Hahn, N.R. Winter, C. Kaehler, D. Emden, R. Leenings, D. Grotegerd, D. Zaremba, Christian Bürger, Katharina Förster, Katharina Dohm, Verena Enneking, Elisabeth J. Leehr, Joscha Böhnlein, Greta Karliczek, Walter Heindel, Harald Kugel, J. Bauer, V. Arolt, and U. Dannlowski. Elevated body-mass

DRAFT

index is associated with reduced white matter integrity in two large independent cohorts. *Psychoneuroendocrinology*, 91(March):179–185, 5 2018. ISSN 03064530. doi: 10.1016/j.psyneuen.2018.03.007.

35. L. Ronan, A.F. Alexander-Bloch, K. Wagstyl, S. Farooqi, C. Brayne, L.K. Tyler, Cam-CAN, P.C. Fletcher, Cam-CAN, and P.C. Fletcher. Obesity associated with increased brain age from midlife. *Neurobiology of aging*, 47:63–70, 7 2016. ISSN 1558-1497. doi: 10.1016/j.neurobiolaging.2016.07.010.
36. M. Rubinov and O. Sporns. Complex network measures of brain connectivity: Uses and interpretations. *NeuroImage*, 52(3):1059–1069, 9 2010. ISSN 10538119. doi: 10.1016/j.neuroimage.2009.10.003.
37. R. Sala-Llonch, C. Junqué, E.M. Arenaza-Urquijo, D. Vidal-Piñeiro, C. Valls-Pedret, E.M. Palacios, S. Domènech, A. Salvà, N. Bargalló, and D. Bartrés-Faz. Changes in whole-brain functional networks and memory performance in aging. *Neurobiology of Aging*, 35(10): 2193–2202, 10 2014. ISSN 01974580. doi: 10.1016/j.neurobiolaging.2014.04.007.
38. R. Sala-Llonch, D. Bartrés-Faz, and C. Junqué. Reorganization of brain networks in aging: a review of functional connectivity studies. *Frontiers in Psychology*, 6(May):1–11, 5 2015. ISSN 1664-1078. doi: 10.3389/fpsyg.2015.00663.
39. J.S. Siegel, B.A. Seitzman, L.E. Ramsey, M. Ortega, E.M. Gordon, N.U.F. Dosenbach, S.E. Petersen, G.L. Shulman, and M. Corbetta. Re-emergence of modular brain networks in stroke recovery. *Cortex*, 101:44–59, 2018. ISSN 19738102. doi: 10.1016/j.cortex.2017.12.019.
40. S.J. Spencer, H. D'Angelo, A. Soch, L.R. Watkins, S.F. Maier, and R.M. Barrientos. High-fat diet and aging interact to produce neuroinflammation and impair hippocampal- and amygdalar-dependent memory. *Neurobiology of Aging*, 58:88–101, 10 2017. ISSN 0197-4580. doi: 10.1016/J.NEUROBIOLAGING.2017.06.014.
41. J.M. Spielberg, N. Sadeh, E.C. Leritz, R.E. McGlinchey, W.P. Milberg, J.P. Hayes, and D.H. Salat. Higher serum cholesterol is associated with intensified age-related neural network decoupling and cognitive decline in early- to mid-life. *Human Brain Mapping*, 38(6):3249–3261, 2017. ISSN 10970193. doi: 10.1002/hbm.23587.
42. O Sporns. Network attributes for segregation and integration in the human brain. *Current opinion in neurobiology*, 1 2013. ISSN 1873-6882; 0959-4388. doi: 10.1016/j.conb.2012.11.015;10.1016/j.conb.2012.11.015.
43. O. Sporns. Structure and function of complex brain networks. *Dialogues in clinical neuroscience*, 15(3):247–262, 9 2013. ISSN 1958-5969.
44. J.R. Tregellas, K.P. Wylie, D.C. Rojas, J. Tanabe, J. Martin, E. Kronberg, D. Cordes, and M.A. Cornier. Altered Default Network Activity in Obesity. *Obesity (Silver Spring, Md.)*, 19 (21):2316–2321, 6 2011. ISSN 1930-7381; 1930-7381. doi: 10.1038/oby.2011.119.
45. I.P. Tzanetakou, N.L. Katsilambros, A. Benetos, D.P. Mikhailidis, and D.N. Perrea. "Is obesity linked to aging?": adipose tissue and the role of telomeres. *Ageing research reviews*, 11(2): 220–9, 5 2012. ISSN 1872-9649.
46. M.N. Valcarcel-Ares, Z. Tucsek, T. Kiss, C.B. Giles, S. Tarantini, A. Yabluchanskiy, P. Balasubramanian, T. Gautam, V. Galvan, P. Ballabh, A. Richardson, W.M. Freeman, J.D. Wren, F. Deak, Z. Ungvari, and A. Csiszar. Obesity in Aging Exacerbates Neuroinflammation, Dysregulating Synaptic Function-Related Genes and Altering Eicosanoid Synthesis in the Mouse Hippocampus: Potential Role in Impaired Synaptic Plasticity and Cognitive Decline. *The Journals of Gerontology: Series A*, 74(3):290–298, 2 2019. ISSN 1079-5006. doi: 10.1093/gerona/gly127.
47. M.P. van den Heuvel and O. Sporns. Network hubs in the human brain. *Trends in cognitive sciences*, 17(12):683–96, 12 2013. ISSN 1879-307X. doi: 10.1016/j.tics.2013.09.012.
48. K.H. Wade, D. Carslake, N. Sattar, S.G. Davey, and N.J. Timpson. BMI and Mortality in UK Biobank: Revised Estimates Using Mendelian Randomization. *Obesity*, 26(11):1796–1806, 11 2018. ISSN 1930-7381. doi: 10.1002/oby.22313.
49. Y.F. Wang, X.M. Ji, G.M. Lu, and L.J. Zhang. Resting-state functional MR imaging shed insights into the brain of diabetes. *Metabolic Brain Disease*, 5(31):993–1001, 2016. doi: 10.1007/s11011-016-9872-4.
50. D. Wechsler. *WAIS III. Escala de Inteligencia de Wechsler para adultos III (adaptación española ed.).* TEA Editores S.A., Madrid, 1999.
51. D. Wechsler. *WISC-IV: Escala de Inteligencia de Wechsler para Niños-IV (2da edición).* TEA Editores S.A., Madrid, 2007.
52. G.S. Wig. Segregated Systems of Human Brain Networks. *Trends in Cognitive Sciences*, 21(12):981–996, 2017. ISSN 1879307X. doi: 10.1016/j.tics.2017.09.006.
53. World Health Organization. BMI classification, 2012.
54. World Health Organization. World Report on Ageing and Health. Technical report, 2015.
55. World Health Organization. Obesity: Data and statistics. Technical report, 2017.
56. R. Zhang, F. Beyer, L. Lampe, T. Luck, S.G. Riedel-Heller, M. Loeffler, M.L. Schroeter, M. Stumvoll, A. Villringer, and A.V. Witte. White matter microstructural variability mediates the relation between obesity and cognition in healthy adults. *NeuroImage*, 172(February): 239–249, 2018. ISSN 10959572. doi: 10.1016/j.neuroimage.2018.01.028.

DRAFT

Supplementary Material

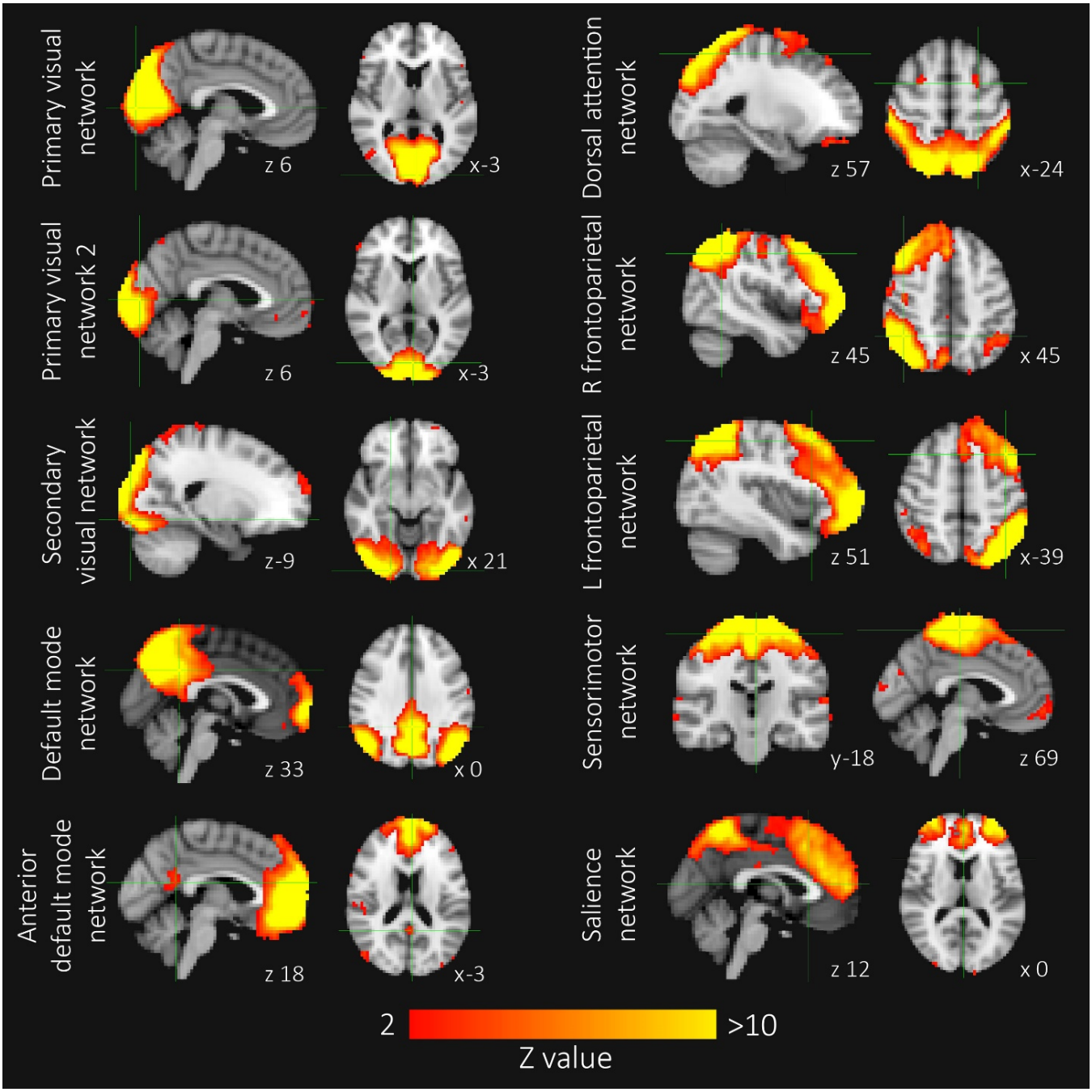

Supplementary Figure 1. Plots disclose the spatial maps corresponding to 10 networks of interest characterized through independent component analysis. The x, y or z MNI coordinates of the slices shown are indicated. In coronal and axial slices, the right hemisphere is displayed on the left side of the image. R: right; L: left.

Primary visual network					
Cun_L_5_2	Cun_L_5_4	Cun_L_5_5	Cun_R_5_2	Cun_R_5_3	Cun_R_5_5
sOcG_L_2_1	sOcG_R_2_1				
Primary visual network 2					
Cun_L_5_1	Cun_L_5_3	Cun_R_5_1	OcG_R_4_3		
Secondary visual network					
FuG_L_3_2	FuG_R_3_2	OcG_L_4_1	OcG_L_4_2	OcG_L_4_3	OcG_L_4_4
OcG_R_4_1	OcG_R_4_2	OcG_R_4_4	sOcG_L_2_2		
Anterior default mode network					
CG_L_7_7	CG_R_7_7	OrG_L_6_1	OrG_L_6_4	OrG_R_6_1	SFG_L_7_3
SFG_L_7_7	SFG_R_7_7				
Dorsal attention network					
IPL_L_6_1	IPL_R_6_1	IPL_R_6_3	ITG_L_7_5	ITG_R_7_2	ITG_R_7_5
sOcG_R_2_2	SPL_L_5_1	SPL_L_5_2	SPL_L_5_4	SPL_R_5_1	SPL_R_5_2
SPL_R_5_3	SPL_R_5_5				
Default mode network					
CG_L_7_1	CG_R_7_1	IPL_L_6_5	IPL_R_6_5	Pcun_L_4_1	Pcun_L_4_3
Pcun_L_4_4	Pcun_R_4_1	Pcun_R_4_3	Pcun_R_4_4	pSTS_L_2_2	
Left frontoparietal network					
IFG_L_6_1	IFG_L_6_2	IFG_L_6_3	IFG_L_6_4	IFG_L_6_6	IPL_L_6_2
ITG_L_7_2	ITG_L_7_6	MFG_L_7_2	MFG_L_7_4	MFG_L_7_5	MFG_L_7_6
OrG_L_6_2	OrG_L_6_3	OrG_L_6_6	SFG_L_7_2	SPL_L_5_5	
Right frontoparietal network					
IFG_R_6_2	IFG_R_6_3	IPL_R_6_2	ITG_R_7_6	MFG_R_7_4	MFG_R_7_5
MFG_R_7_6	MTG_R_4_1	OrG_R_6_2	OrG_R_6_3	OrG_R_6_6	SFG_R_7_2
SFG_R_7_3					
Salience network					
CG_L_7_3	CG_R_7_3	IPL_L_6_3	IPL_L_6_4	IPL_R_6_4	MFG_L_7_1
MFG_L_7_3	MFG_R_7_1	MFG_R_7_3	PCL_R_2_1	Pcun_L_4_2	SFG_L_7_1
SFG_L_7_6	SFG_R_7_1	SFG_R_7_6	SPL_L_5_3		
Sensorimotor network					
PCL_L_2_1	PCL_L_2_2	PCL_R_2_2	Pcun_R_4_2	PoG_L_4_4	PoG_R_4_4
PrG_L_6_3	PrG_L_6_4	PrG_R_6_2	PrG_R_6_3	PrG_R_6_4	SFG_L_7_4
SFG_L_7_5	SFG_R_7_4	SFG_R_7_5	SPL_R_5_4		
Medial temporal network					
Amyg_L_2_1	Amyg_L_2_2	Amyg_R_2_1	Amyg_R_2_2	Hipp_L_2_1	Hipp_L_2_2
Hipp_R_2_1	Hipp_R_2_2				
Striatal thalamic network					
Str_L_6_1	Str_L_6_2	Str_L_6_3	Str_L_6_4	Str_L_6_5	Str_L_6_6
Str_R_6_1	Str_R_6_2	Str_R_6_3	Str_R_6_4	Str_R_6_5	Str_R_6_6
Tha_L_8_1	Tha_L_8_2	Tha_L_8_3	Tha_L_8_4	Tha_L_8_5	Tha_L_8_6
Tha_L_8_7	Tha_L_8_8	Tha_R_8_1	Tha_R_8_2	Tha_R_8_3	Tha_R_8_4
Tha_R_8_5	Tha_R_8_6	Tha_R_8_7	Tha_R_8_8		

Supplementary Table 1. Brainnetome atlas regions (http://atlas.brainnetome.org/) assigned to each of the 12 brain networks of interest.

DRAFT

	OB adult	HW adult	Senior	OB young	HW young
Modularity	0.58	0.09	-0.15	-0.03	-0.52
	(0.75)	(1.09)	(0.74)	(1.06)	(1.04)
Path length	0.39	0.31	0.37	-0.39	-0.76
	(0.59)	(0.64)	(0.99)	(1.15)	(1.02)
Mean degree	-0.50	-0.07	-0.04	-0.02	0.66
	(0.44)	(0.79)	(0.64)	(0.91)	(1.56)
Mean strength	-0.48	0.11	0.04	-0.13	0.47
	(0.60)	(1.06)	(0.86)	(0.91)	(1.26)

Supplementary Table 2. Mean and standard deviation of graph-based parameters across groups (z-scores; adjusted for mean translational movements). OB = Participants with obesity, HW = Healthy-weight individuals.

DRAFT